AIAA JOURNAL
Vol. 45, No. 12, December 2007

Dual-Pump Coherent Anti-Stokes Raman Scattering Thermometry in Heavily Sooting Flames

Sean P. Kearney*
Sandia National Laboratories, Albuquerque, New Mexico 87185
and
Matthew N. Jackson†
Texas Technical University, Lubbock, Texas 79409

DOI: 10.2514/1.31054

We investigate the utility of dual-pump coherent anti-Stokes Raman scattering of N_2 for the probing of rich acetylene- and ethylene-fueled flames with soot volume fractions upwards of 2 ppm, which is well in excess of recent reports of sooting flame measurements with the dual-pump approach. A substantial level of interference in the coherent-Raman spectra is observed when the N_2 Q-branch signature is positioned in spectral regions that have been reported to be interference-free and are removed from the peaks of the C_2 Swan system that are the chief obstacle to thermometry in sooting flames. This interference is attributed to coherent-Raman processes in laser-produced C2 and in olefinic hydrocarbons, which exhibit Raman frequencies that are resonant with the pump-2/Stokes frequency difference. A second source of coherent interference is also discussed, in which a significant nonresonant pedestal is added to the coherent-Raman signal, presumably as a result of laser-induced breakdown in the presence of only the highest soot loadings probed here. Two "spectrally quiet" regions for the coherent-Raman signal near 483 and 496 nm are identified, and temperature profiles from an array of heavily sooting acetylene-fueled nonpremixed flames and a premixed ethylene/air flame are provided using a N_2 Q-branch signature positioned near 483 nm. The results show that dual-pump coherent anti-Stokes Raman scattering of N_2 is a viable thermometer at soot loadings at least as high as 2 ppm, albeit with more restrictions on the spectral position of the signal than previously thought.

Introduction

LASER-DIAGNOSTIC approaches for combustion measurements have seen an explosion in their development over the last three decades [1,2]. These optical approaches are noninvasive, provide very fine spatial and temporal resolution, and yield information about virtually any parameter of interest. Although a multitude of laser-based techniques have proven successful for the probing of clean, particulate-free laboratory flames, the majority of these approaches are of limited utility in particle-laden, luminous flames, in which optical interferences overwhelm the diagnostic signatures of interest.

Coherent anti-Stokes Raman scattering (CARS) is one exception, because its laserlike and blue-shifted signal permits efficient spatial and spectral discrimination against incoherent optical interferences resulting from soot scattering and emission, laser-induced soot incandescence, and polycyclic aromatic hydrocarbon fluorescence. Early investigations of N_2 CARS thermometry in sooting flames [3–6] used a frequency-doubled Nd:YAG laser to provide degenerate pump photons to the CARS process and to pump the Stokes dye source. This approach yields a nitrogen CARS signal near 473 nm, which, unfortunately, is in resonance with the $\Delta v = +1$ band of the $d^3\pi_g - a^3\pi_u$ Swan system‡ of the C_2 molecule that is produced by laser-induced vaporization of soot. This resonance often leads to incoherent absorptive [5,8] and emissive [3] interference with the CARS spectral signature, and coherent interference resulting from Raman-resonant and electronic-resonance-enhanced (ERE) CARS of C_2 has also been reported [3,9,10].

More recently, techniques that shift the CARS signal from sooty flames to an interference-free portion of the spectrum have been demonstrated. These include pure-rotational CARS [11], dual-pump CARS [12–14], and spectrally shifted vibrational CARS [15,16]. At flame temperatures, the pure-rotational CARS approach has been demonstrated to be less accurate than vibrational CARS [17], and analysis of pure-rotational CARS spectra can be complicated by overlapping lines from the multiple hydrocarbon and product species found in fuel-rich flames. With dual-pump CARS, one of the frequency-degenerate pumps from the Nd:YAG laser is replaced by a laser beam from a tunable-dye source. The wavelength of this second pump source can be scanned to shift the CARS signal away from the C_2 Swan bands and/or to probe multiple species with a single CARS instrument [18]. Dual-pump CARS has recently been demonstrated in sooting ethylene–air flames [12,14], and an improvement in accuracy vis-à-vis degenerate-pump CARS was quantified for soot volume fractions up to ~0.6 ppm, for which bias errors were in excess of 150 K when degenerate Nd:YAG pumps were used [14]. Shifted vibrational CARS of nitrogen has also been demonstrated [15,16], in which two degenerate pump photons from a tunable-dye source are used with a broadband Stokes laser. The tuning of both pump beams then serves to shift the CARS signal. Relative to dual-pump CARS, shifted vibrational CARS may result in spectra that are simpler to interpret, but the ability to probe multiple species is lost and the multimode nature of the two pump beams may degrade the precision of single-shot measurements.

In this paper, we discuss dual-pump CARS investigations of heavily sooting flames employing both acetylene and ethylene fuels.

Presented as Paper 432 at the 44th AIAA Aerospace Sciences Meeting and Exhibit, Reno, NV, 9–12 January 2006; received 15 March 2007; accepted for publication 15 August 2007.

*Principal Member of the Technical Staff, Engineering Sciences Center, P.O. Box 5800, Mail Stop 0834; spkearn@ sandia.gov. Member AIAA (Corresponding Author).

†Department of Mechanical Engineering; currently Senior Member of the Technical Staff, Monitoring Systems and Technology Center, Sandia National Laboratories, Albuquerque, NM 87185.

‡There appears to be some confusion in the literature regarding the electronic-state designations for C_2. Much of the combustion diagnostics literature refers to the Swan system as $A^3\Pi_g - X^3\Pi_u$. Eckbreth [1] notes that, "the true lowest lying ground state was discovered only after a slightly higher energy level was assigned as the X state;" whereas Herzberg [7] assigns the Swan system as $d^3\pi_g - a^3\pi_u$, leaving the X designation to the lowest energy level. We used the $d - a$ designation here, but point out this discrepancy.

This extends the application of dual-pump CARS to significantly higher soot loadings and to fuels other than the ethylene–air flames of sub-ppm soot volume fraction [12,14] and the JP-8 combustor studies [13] that have been the subject of recent reports. We discuss our observations of coherent interference from additional Raman processes in laser-produced C_2 and olefinic hydrocarbons, seen at N_2 CARS-signal wavelengths previously identified to yield usable spectra from sooting flames [12,14–16], as well as an additional type of interference in which a strong nonresonant pedestal is added to the N_2 CARS signal at very-high-soot loadings. CARS-measured temperatures obtained with a pump-2 wavelength of 544.5 nm (CARS signal near 483 nm) are presented alongside measured soot volume fractions in an attempt to assess the magnitude of soot volume loadings for which dual-pump CARS is applicable. The results demonstrate that dual-pump CARS temperatures may reliably be obtained for soot loadings of at least 2 ppm in fuel-rich premixed and diffusion flames.

Fuel-Rich Flame Structure and Soot Volume Loadings

Two types of fuel-rich sooting flames have been investigated, as shown in Figs. 1 and 2: 1) a nonpremixed burner, which provided an array of N_2-diluted C_2H_2-fueled diffusion flames and 2) a more spatially uniform, premixed C_2H_4/air flame stabilized on a standard porous-plug McKenna burner, which was studied to provide a consistent link to earlier dual-pump CARS investigations using C_2H_2 fuel in this burner [12,14]. The nonpremixed burner is shown in Fig. 1, with a three-dimensional rendering of the burner tube routings provided in Fig. 1a and the burner-surface tube configuration shown in Fig. 1b. The burner was designed to simulate the products of aluminum-based propellant combustion using gas-phase reactants and is based on an arrangement of alternating fuel and oxidizer tubes of 3.17-mm diameter. As seen in Fig. 1b, three ports for controlled injection of micron-scale aluminum particles are provided near the center of the burner. For the experiments reported here, aluminum particles were not injected into the burner flow. We instead concentrated on the utility of our dual-pump CARS instrument for probing heavily sooting nonpremixed flames. Acetylene, which was diluted with nitrogen, was used as the fuel, with total gas flow rates of 4, 15, and 5 SLPM for C_2H_2, N_2, and O_2, respectively. The total N_2 flow was split nominally 50/50 between the fuel and oxidizer streams. The diffusion flames were laminar, with steady conditions near the center of the burner and close to the burner surface. More flickering conditions existed toward the burner edges and higher up in the flame array.

Laser-induced-incandescence (LII) [19] images of soot structure in the diffusion-flame array are provided in Fig. 3. Details of our LII system can be found elsewhere [20]. The LII images in Fig. 3 clearly show the structure of the burner flow to be an array of sooting fuel jets surrounded by coflowing oxidizer streams, and the results are useful for quantifying the soot loadings in the CARS measurements reported here. Three vertical-axis temperature profiles are reported with the CARS probe volume positioned above 1) a fuel port near the edge of the flame, where soot loadings were highest, 2) an adjacent oxidizer port, and 3) an Al-injection port at the center of the burner, to which no flow was supplied. The locations for the vertical-axis CARS scans are highlighted in Fig. 1b and shown by the white vertical arrows in Fig. 3.

Our LII measurements were calibrated for soot volume fraction against HeNe-laser extinction data acquired in the same $C_2H_2/N_2/O_2$ flame array. We used a value of $K_e = 9$ for the extinction coefficient of soot used to deduce the soot volume fraction f_v from our light-extinction data [20]; this value is taken from recent measurements from both postflame and in-flame soot, which report K_e between 8 and 10 for a variety of fuels in laminar and turbulent flames [21]. Earlier measurements of the soot refractive index, such as by Dalzell and Sarofim [22], are commonly used for interpretation of light-extinction data, but yield much lower K_e values that result in soot volume fractions that are almost a factor of 2 higher when used for the interpretation of light-extinction data. We believe the more recent evidence for higher K_e values to be quite convincing and have

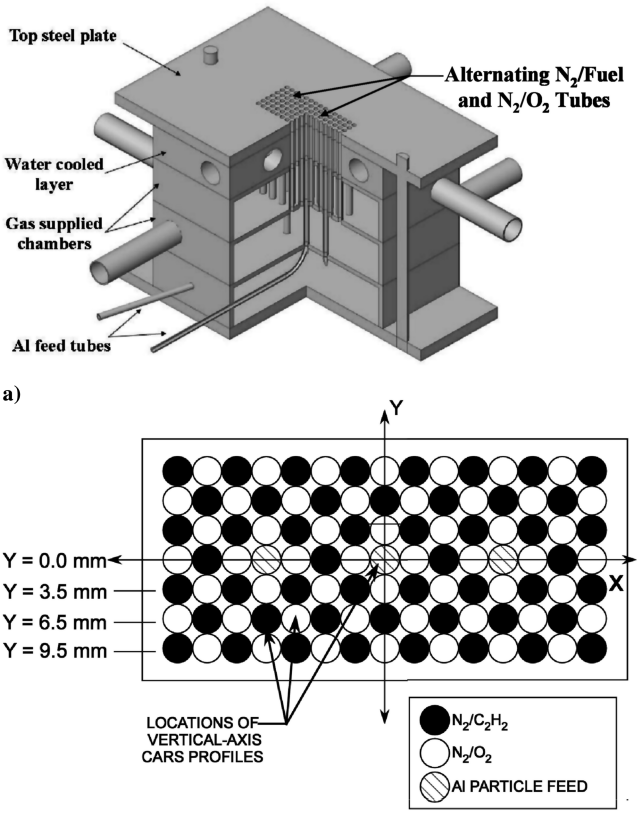

Fig. 1 Propellant simulating burner facility: a) 3-D-rendered drawing of the burner and b) arrangement of the fuel and oxidizer tubes. All tubes are 3.17 mm in diameter.

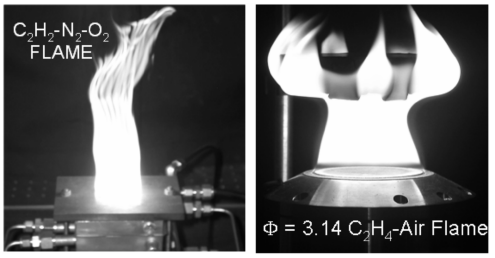

Fig. 2 Digital photographs of the two fuel-rich heavily sooting flames probed by dual-pump CARS.

employed this value here. This results in lower calibrated LII volume fractions, such that the soot volume loadings for the successful dual-pump CARS application reported here are conservative. LII-measured profiles of soot volume fraction to be presented alongside our CARS temperature data are estimated to be +20 to −40% uncertain, subject to the assumption that K_e does indeed lie in the 8–10 range of recent measurements. This uncertainty estimate is based on the combined effects of uncertainty in the light-extinction calibration, absorption of the LII probe laser, and trapping of the LII signal by absorbing soot between the probe laser sheet and detector.

A second set of CARS measurements was carried out in a premixed C_2H_4/air flat flame, using a water-cooled porous-plug McKenna burner of 50-mm diameter. Reactant flows of 1.8 SLPM C_2H_4 and 8.2 SLPM of filtered dry air were used to provide a fuel-rich flame with an equivalence ratio $\Phi = 3.1$. A 76-mm-diam× 12.5-mm-thick steel stabilization plate was positioned 50 mm above the burner surface to minimize flickering of the premixed flame. A shroud flow of 16 SLPM of air further stabilized the flame environment with the addition of a diffusion flame around the edges of the burner. A digital photograph of the premixed flame is provided in Fig. 2, in which the structure of the flame is clearly shown by

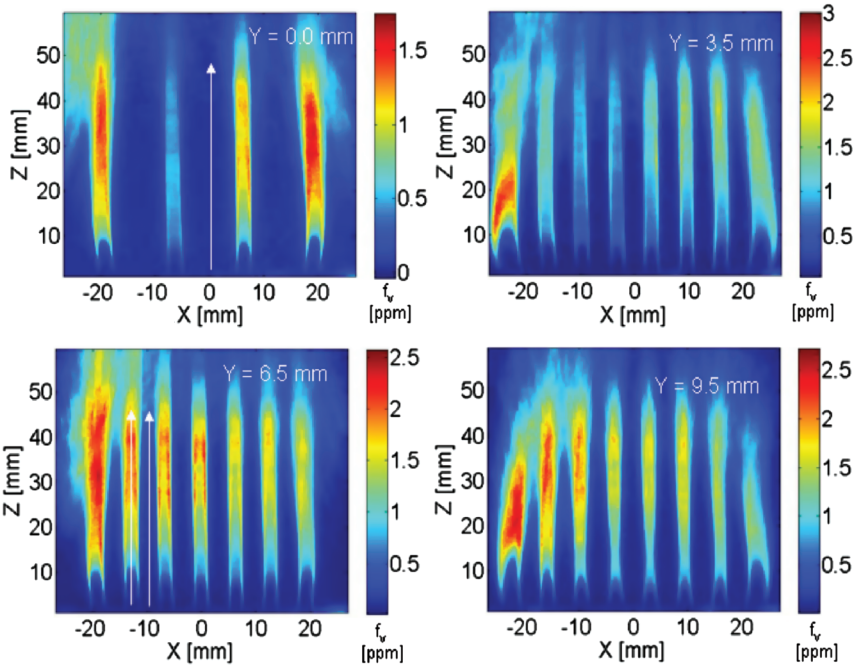

Fig. 3 Soot-volume-fraction images in the propellant simulating burner of Fig. 1, as measured by LII at selected Y equal to constant planes. The LII images were averaged for 150 laser shots. The white arrows in the figure indicate the position of the CARS probe volume for the vertical-axis temperature profiles reported in this paper.

intense luminosity from soot. Vertical profiles of soot volume fraction in this flame were quantified by extinction of HeNe-laser radiation along a path through the centerline of the circular-plan burner. The impact of spatial averaging in the path-integrated extinction measurement was neglected, because this type of flat flame displays a nearly one-dimensional structure, which was confirmed by qualitative LII images. Peak extinction-measured soot volume fractions in this flame approached 0.8 ppm with an uncertainty that was conservatively estimated at $\pm 30\%$, which was primarily a result of the spread in recent measurements of soot K_e and the observed variations in our raw light-extinction data.

Dual-Pump CARS Instrument

Energy-Level Diagrams

Energy-level diagrams for conventional N_2 CARS using frequency-degenerate 532-nm pump beams and a dual-pump CARS process with nondegenerate pumps are provided in Fig. 4. In both cases, the difference, $\omega_1 - \omega_S$, between the pump 1 and Stokes frequencies is tuned to drive a Raman Q-branch polarization in N_2, which scatters the incident pump-2 radiation at ω_2 to yield a CARS signal at $\omega_{\mathrm{CARS}} = (\omega_1 - \omega_S) + \omega_2$. In the case of conventional N_2 CARS, the resulting CARS signal is degenerate with the peak of the $\Delta v = +1 C_2$ Swan band near 473 nm, as shown by the computed C_2 emission spectra from Shaddix and Smyth [23] contained in Fig. 5. Significant interference with the CARS signal may occur in this case. With a tunable pump-2 source, the CARS-signal frequency may be shifted arbitrarily to a location away from these strong C_2 interferences. We selected a pump-2 wavelength of $\lambda_2 = 544.5$ nm, which shifts the bandhead of the resulting N_2 CARS signal to $\lambda_{\mathrm{CARS}} = 483.2$ nm, away from the peaks of the C_2 Swan system and from additional interference encountered in the fuel-rich heavily sooting flames. The details of the observed interference and selection of the pump-2 wavelength are presented later.

Optical System Layout

The dual-pump CARS instrument used for the sooting flame investigations is presented schematically in Fig. 6. A frequency-doubled Q-switched Nd:YAG laser (Spectra Physics Pro-350) operating at 10 Hz provides 1200 mJ of 532-nm radiation per 12-ns

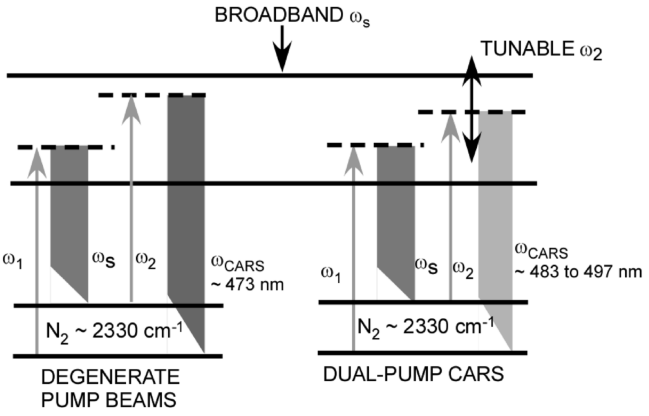

Fig. 4 Energy-level diagrams for conventional and dual-pump CARS processes.

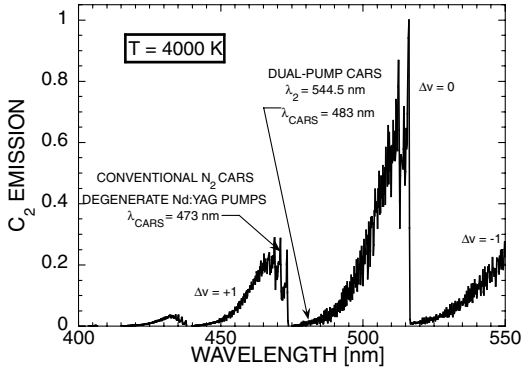

Fig. 5 Swan-band spectrum of C_2 as computed by Shaddix and Smyth [23] for $T = 4000$ K, near the vaporization point of soot. The nominal spectral locations for conventional N_2 CARS with degenerate Nd:YAG pumps and dual-pump CARS with a pump-2 wavelength of 544.5 nm are shown. Use of the dual-pump technique moves the CARS-signal beam away from C_2 spectral interferences.

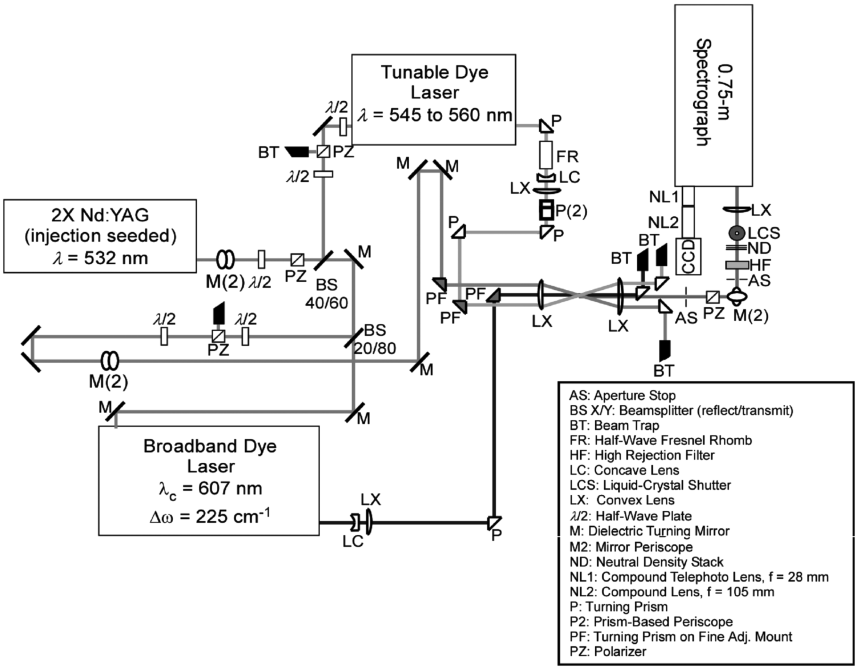

Fig. 6 Dual-pump CARS instrument for probing of heavily sooting flames.

laser pulse. With injection seeding, the Nd:YAG source has a near-transform-limited line width of 0.003 cm^{-1}. The Nd:YAG system provides sufficient energy to pump both the narrowband tunable-dye laser and the broadband Stokes dye source while providing the pump-1 beam to the CARS process. The in-house-built Stokes dye laser uses side-pumped Bethune-type prisms [24] for the oscillator and amplifier dye cells. The Stokes laser is operated in multimode to maximize its energy output. A mixture of Rhodamine 610 and Rhodamine 640 in methanol provides a Stokes output centered at 607 nm with a nominal bandwidth of 225 cm^{-1} (full-width half-maximum), as measured by fits to nonresonant CARS spectra obtained from argon. The narrowband dye source (Continuum ND6000) uses Fluoroscein 548 dye with a NaOH base in methanol, to provide tunable pump-2 radiation over a 543- to 560-nm range with a 0.1 cm^{-1} manufacturer-specified line width. Nominal beam energies are 45, 35, and 25 mJ/pulse for the pump-1, pump-2, and Stokes sources, respectively.

The parallel-polarized pump and Stokes beams are focused in a folded BOXCARS [25] configuration by a $f = 500$-mm spherical singlet lens and recollimated using a $f = 1000$-mm singlet. The diameter of the ellipsoidal CARS probe volume was 50–100 μm, with 80% of the CARS signal generated in a 2.25-mm axial beam-overlap region, as determined by monitoring the intensity of the nonresonant CARS signal generated in a glass cover slip that was translated through the beam-overlap region. The resulting blue-shifted CARS-signal beam was relayed to a 0.75-m spectrograph with a 1200 l/mm grating that dispersed the CARS signal onto a back-illuminated CCD camera. A magnification of 3.75 at the CCD focal plane was provided by the relay lens pair at the exit of the spectrograph, which resulted in a detection system dispersion of 0.17 cm^{-1}/pixel and a spectral resolution of 0.57 cm^{-1} for the CARS instrument.

Rejection of intense background thermal radiation from the white-hot C_2H_2-fueled flames was provided by placing a polarizer and apertures in the CARS beam path and by using a liquid-crystal shutter with a contrast on the order of 10^3 to gate the detection system to 70 μs per laser pulse. The liquid-crystal shutter was crucial to the feasibility of these measurements, because intense luminous background from the flames overwhelmed the CARS signal without it.

Fitting of N_2 CARS Spectra for Temperature

CARS spectra were averaged on the detector for 10 laser shots, with 10 shot-averaged spectra recorded at each measurement location. Optical background was recorded with the Stokes beam blocked and was subtracted from all spectra. The background-corrected data were then normalized by shot-averaged nonresonant CARS spectra from argon to correct for the average shape of the Stokes dye-laser spectrum. Temperatures were derived from processed N_2 CARS spectra using the CARSFT code, originally developed by Sandia National Laboratories [26]. CARSFT computes theoretical CARS spectra and uses a nonlinear optimization routine to find the best fit to the experimental data. The dual-pump CARS convolution equations used by CARSFT are summarized by Hancock et al. [27]. In our experiments, the Stokes dye-laser envelope overlapped both N_2 Q-branch and H_2 pure-rotational S-branch transitions. Both of these gases were included in the theoretical calculations, although fitting was restricted to the spectral region containing only the first two vibrational levels of N_2. The instrument resolution (CARSFT probe line width) was fixed at the 0.57 cm^{-1} value measured for the CARS system, and the theoretical susceptibility was convolved with both the pump-2 laser line width (0.1 cm^{-1}) and the instrument function. Convolutions with the pump-1 and Stokes laser profiles were not required, because the injection-seeded pump-1 line width was much narrower than the probed Raman lines and because the spectra were normalized by measured Stokes laser profiles. The H_2 mole fraction was fixed at representative levels based on more time-consuming fits to the full CARS spectrum at selected locations. Exact fitting of the hydrogen mole fraction was not required, because it did not significantly impact the resulting N_2 CARS temperatures.

Along with the temperature, the fitting routine varies horizontal and vertical shift parameters to compensate for uncertainty in the spectrograph dispersion and optical background subtraction. The routine also varies the nitrogen mole fraction in a restricted range to adjust the relative importance of the nonresonant contribution to the CARS spectrum in the fuel-rich hydrocarbon flames probed here, for which the nonresonant susceptibility is uncertain. This procedure is valid provided that absolute species mole-fraction measurements are not required. A nonresonant susceptibility of 12.5×10^{-18} cm^3/erg-amagat was used for the C_2H_4/air premixed flame. This value was computed using measured product-gas concentrations by Xu et al. [28] for a $\Phi = 2.94$ C_2H_4/air flame on a McKenna burner. For the nonpremixed C_2H_2-fueled flames, a nonresonant background susceptibility of 17×10^{-18} cm^3/erg-amagat was used to fit spectra obtained from the oxidizer jet and above the Al-injection port at the burner center, because this value is representative of the combustion products for the $C_2H_2/O_2/N_2$ mixture employed, as computed using

the NASA equilibrium code [29]. The nonresonant susceptibility of acetylene, 50×10^{-18} cm^3/erg-amagat [30], was used to fit the data from the C_2H_2 fuel jet.

Interference Observed in Dual-Pump CARS Spectra

Coherent Interference from Raman-Resonant Processes

Dual-pump CARS spectra obtained from the C_2H_2 fuel jet and premixed C_2H_4/air flame are shown in Fig. 7. Both spectra were obtained with a pump-2 wavelength of 556.8 nm. The Q branch of N_2 and the H_2 pure-rotational $S(5)$ signature are observed along with additional features that present interference to N_2 CARS thermometry. The interference is coherent in nature; it disappears when any one of the pumps or the Stokes laser beam is blocked, and it has the same polarization state as the Raman-resonant N_2/H_2 features. The appearance of the interference spectrum is intimately connected to the presence of soot in the CARS probe volume. Interference is not present in flames that do not produce visible luminosity from soot, and the amplitude of the interference peaks noticeably increases with the measured soot volume fraction. Incipient interference appears in the $\Phi = 3.1$ C_2H_4/air flame at a height just below which measurable soot appears and was also observed in weakly sooting C_2H_4/air flames for Φ as low as 2.3. The magnitude of the interference peaks is considerably larger in the C_2H_2 fuel jet, in which maximum soot volume fractions were in excess of 2.0 ppm, than in the premixed C_2H_4/air flame, which had a maximum soot volume loading of 0.8 ppm.

The interference spectrum is a result of coherent-Raman processes in laser-produced C_2 and perhaps from olefinic hydrocarbon species, for which the C = C double bonds are Raman-active near 1650 cm^{-1} [7,31]. The location of the interference peaks remains essentially stationary as λ_2 is scanned from 555 to 560 nm, confirming that a Raman polarization at $\omega_2 - \omega_S \sim$ 1500–1650 cm^{-1} is responsible for their generation. The difference frequency, $\omega_2 - \omega_S$, is plotted at the top of Fig. 7 to clarify the Raman frequencies of the observed interference. The position of the interference peaks directly corresponds to the Raman Q-branch frequencies of C_2 in the $a^3\pi_u$ electronic state for $v'' = 0$ and 1. There is lessened agreement of the data with known C_2 Raman frequencies at $v'' = 2$ and 3, so that some uncertainty remains in the assignment of these peaks, which we suggest are still a likely result of C_2 or unburned olefinic hydrocarbons.

In the flames investigated here, the concentration of laser-produced C_2 and olefinic fuels is on the order of a few percent or less,[§] and ordinary Raman-resonant processes are likely not sufficient to generate the large-amplitude signatures seen in Fig. 7. The coherent-Raman interferences may well be augmented by their spectral proximity (within 1000 cm^{-1}) to the $\Delta v = +1$ and $\Delta v = 0$ features of the C_2 Swan system, which can enhance the nonlinear susceptibility for CARS of C_2 via well-known electronic-resonance enhanced (ERE) CARS processes [9,33]. Eckbreth et al. [10] reported ERE CARS of laser-produced C_2 in their dual-Stokes CARS measurements in fuel-rich flames, in which the C_2 signatures at Raman shifts near 1618 cm^{-1} were within 700 cm^{-1} of the $\Delta v = +1$ Swan transitions.

Suitable spectral locations for the N_2 CARS signal were determined by scanning the CARS wavelength through the region between the $\Delta v = +1$ and $\Delta v = 0$ Swan bands shown in Fig. 5. A series of dual-pump CARS spectra obtained from the C_2H_2 fuel jet at a height of 21 mm above the burner surface is shown in Fig. 8. The LII-measured soot volume fraction at this location was 1.4 ppm and the CARS-measured temperature was 2000 K. The spectra were

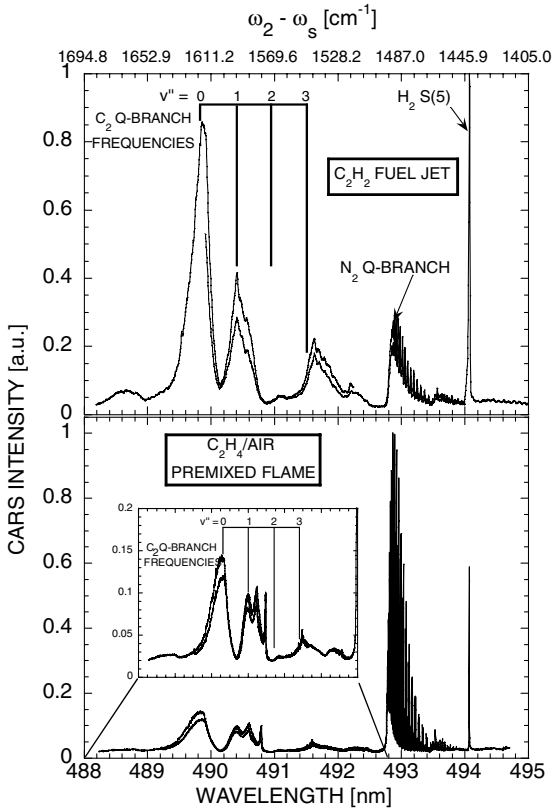

Fig. 7 Dual-pump CARS spectra recorded in sooting flames with the pump-2 wavelength tuned near 556.8 nm. The spectra display the expected contributions from the N_2 Q branch and an isolated pure-rotational S-branch line from H_2, along with unexpected coherent interference from C_2 and olefinic hydrocarbons. The position of the strongest interference peaks is found to be coincident with the tuning of the pump-2/Stokes difference frequency $\omega_2 - \omega_s$ to the Raman Q-branch frequencies of C_2, which are indicated in the upper plot.

averaged for 100 laser shots and the nominal wavelength of the CARS-signal beam was shifted from 482.4 nm to 497.7 nm by scanning the pump-2 wavelength from 543 to 563 nm. The spectra at $\lambda_2 = 543$ and 544.5 nm are essentially interference-free, as are the spectra at $\lambda_2 = 560$ and 563 nm. Comparatively, a choice of $\lambda_2 =$ 544.5 nm permits simultaneous measurement of H_2 with N_2-derived temperatures, whereas a choice of λ_2 near 560 nm enables measurement of both H_2 and CO_2 with temperature, as demonstrated by Roy et al. [13]. We selected a pump wavelength of $\lambda_2 = 544.5$ nm, because CO_2 probing was not a requirement; this resulted in simpler CARS spectra in which extensive modeling of CO_2 contributions was not required.

Interference of the type discussed here has not been noted in recent investigations of dual-pump [12,14] and spectrally shifted [15,16] N_2 CARS thermometry in sooting flames. The spectrally shifted CARS technique should not produce the interference seen here, because no pump/Stokes combinations are tuned near 1600 cm^{-1}. Consistent with this, Stricker et al. [15,16] presented spectrally shifted vibrational CARS of N_2 at 487 nm for soot volume loadings up to 0.8 ppm with no reports of interference in their spectra. Recent reports of dual-pump CARS of N_2 in sooting flames also do not note this type of interference, most likely because the flames investigated had less soot than in our study. Beyrau et al. [12] used dual-pump N_2 CARS near 488.5 nm for thermometry in a partially premixed C_2H_4/air flame, for which no soot data were presented. Malarski et al. [14] reported successful dual-pump N_2 CARS thermometry at $\lambda_{CARS} \sim 487$ nm in a premixed C_2H_4/air flame for soot volume loadings as high as 0.6 ppm. More recent investigations by the same research group [34] note a "smeared feature" at Raman shifts from 1580–1630 cm^{-1} in dual-pump CARS spectra from fuel-rich flames, which was attributed to resonant Raman processes in olefinic hydrocarbon species.

[§]The concentration of olefinic hydrocarbons and C_2 is small in sooting regions of these fuel-rich flames. Of the two fuels studied here, C_2H_4 is the only olefinic. Previous investigations [28,32] of fuel-rich premixed C_2H_4 combustion show that olefinic species are present in 0.1% mole fraction or less in sooting regions of the flame, with the most abundant hydrocarbon species being acetylene at several percent volume fraction. Laser-produced C_2 is also a relatively minor species. For a soot volume loading of 2 ppm and a temperature of 2000 K, the estimated C_2 mole fraction for complete conversion of soot mass to C_2 is only 3%.

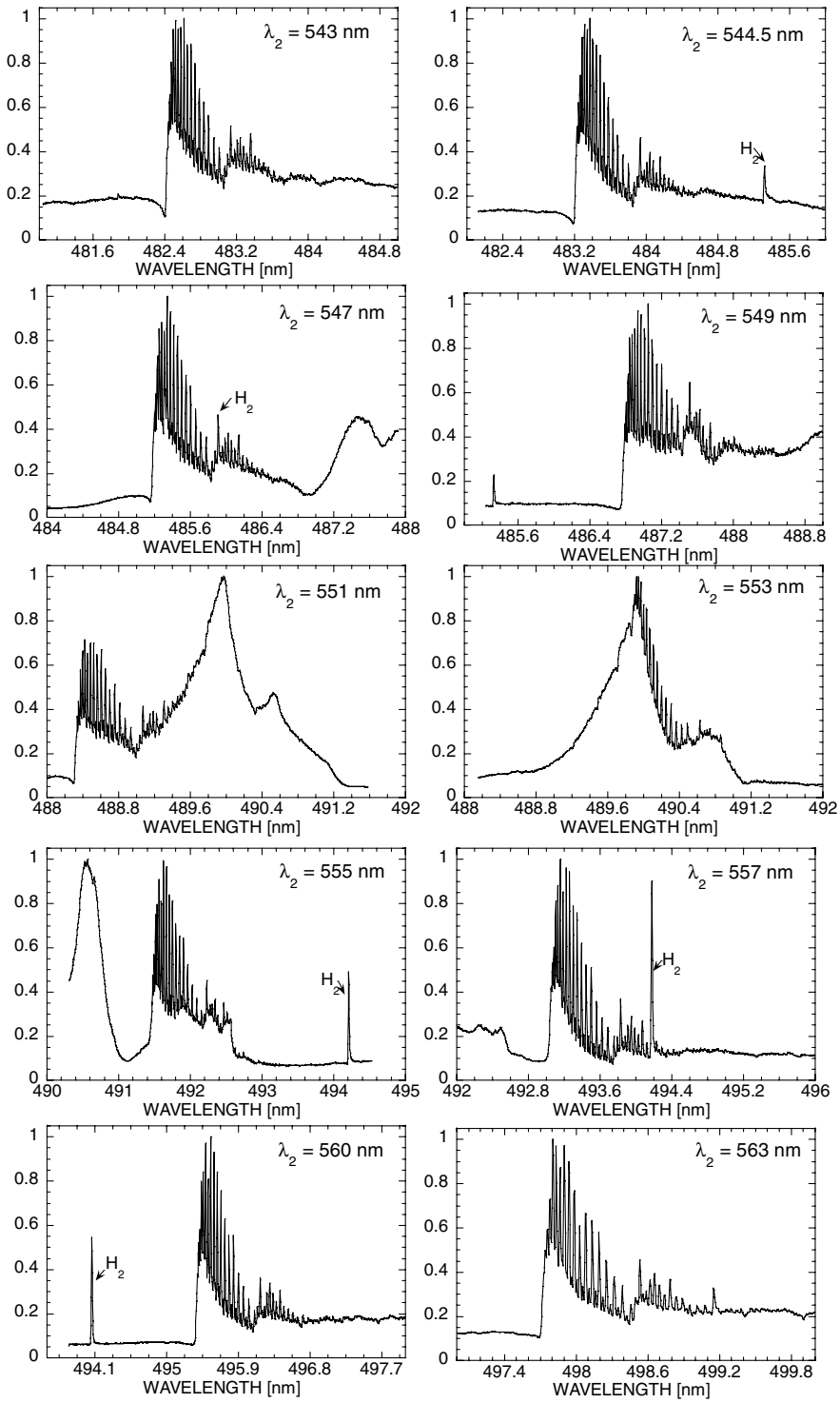

Fig. 8 Dual-pump CARS spectra from a heavily sooting $C_2H_2/N_2/O_2$ flame. The intensity of the CARS signal is plotted on the vertical axis and the spectra have not been corrected for stray-light background. The spectra were averaged for 100 laser shots and the CARS-signal wavelength is shifted in each spectrum by scanning the pump-2 wavelength λ_2.

Coherent Interference from Nonresonant Processes: Laser-Induced Breakdown

Enhanced nonresonant CARS signatures of the type shown in the spectra of Fig. 9 were also observed in a limited number of spectra. This type of interference was only observed in the C_2H_2-fueled flames and was significant only when the soot volume fraction was greater than about 2 ppm. This interference is strikingly similar to that reported by Beiting [35,36] and by Hancock et al. [37] in their CARS measurements in coal-burning flames. The observed offset in the spectrum closely follows the shape of the Stokes dye-laser profile observed in nonresonant CARS spectra recorded in argon. The offset appears as an addition to the N_2 signature and not as a modulated dip of the resonant N_2 signal near the Q-branch bandhead, as typically seen in the presence of significant nonresonant background. Both Beiting [35,36] and Hancock et al. [37] attribute this effect to laser-induced breakdown in the beam-crossing region, which forms a plasma with large nonresonant susceptibility. Reduction of the gas-phase breakdown threshold by particulate is well-established [35], but is not typically observed in sooting flames, in which primary particle sizes are on the order of tens of nanometers [21,38], well below the $\sim$1-μm size [35,36] at which particulate begins to impact the breakdown threshold. Nevertheless, it is possible for soot particle

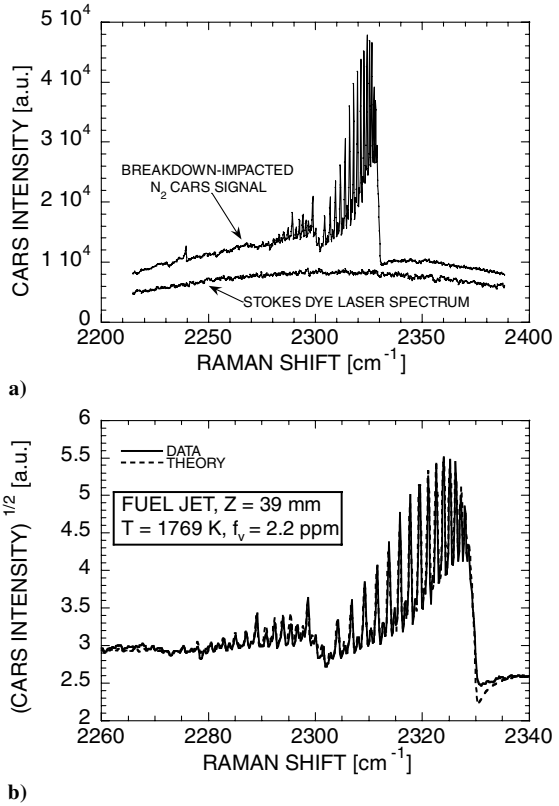

Fig. 9 Example of a CARS spectrum that has been impacted by dielectric breakdown. The spectrum was acquired above the C_2H_2 fuel jet at $z = 39$ mm above the burner surface on which the LII-measured soot volume fraction was 2.2 ppm. This spectrum was obtained with a pump-2 wavelength of 544.5 nm and averaged for 100 laser shots, on some of which a breakdown event occurred: a) a "raw" spectrum, which has not been normalized by the Stokes dye-laser profile and b) processed data and the resulting theoretical fit.

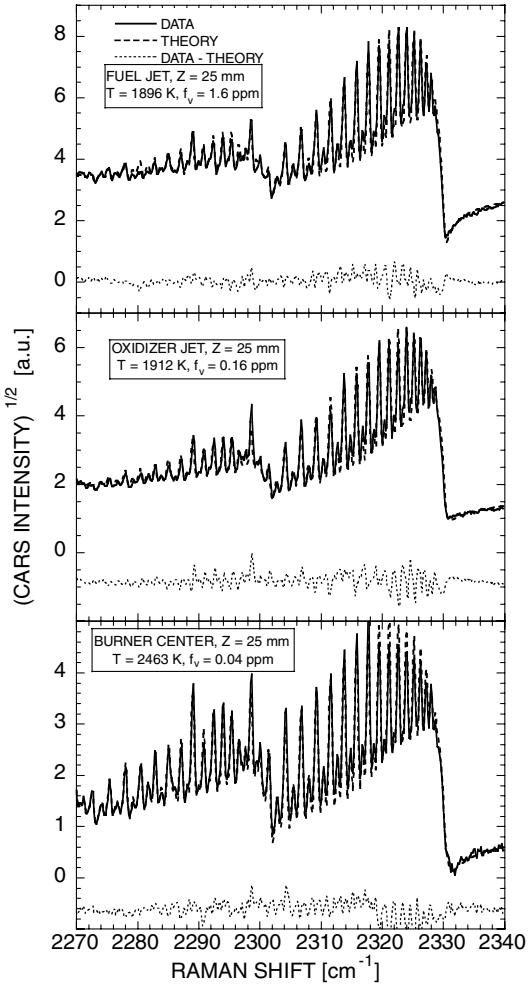

Fig. 10 Sample fits to CARS spectra obtained at $Z = 25$ mm above the burner surface from the fuel jet, oxidizer stream, and above the central Al-particle-feed port of the array of $C_2H_2/N_2/O_2$ diffusion flames.

agglomerates to reach lengths of several hundred nanometers to microns [38], so that laser-induced breakdown may occur under heavy soot loadings of the type encountered in our C_2H_2-fueled flames. In shot-averaged spectra, the impact of this breakdown-type of interference is not too severe, because a breakdown event only occurred on a small fraction of the accumulated laser shots. Normalization of shot-averaged spectra by the measured Stokes laser profile generally removes the Gaussian structure of the offset, and a vertical shift can be added to the theory to obtain reasonable fits to the data, as shown in the processed spectrum provided in Fig. 9b. Single-laser-shot spectra are more severely impacted, because the enhanced nonresonant pedestal often overwhelms smaller single-pulse N_2 signals.

Nitrogen CARS Thermometry Results

Shot-Averaged Data

Representative fits to CARS spectra obtained from the $C_2H_2/O_2/N_2$ flame array at a height of $Z = 25$ mm above the burner surface in the fuel jet, oxidizer stream, and dormant Al-particle injection ports are provided in Fig. 10. Each of these spectra was averaged on the detector for 10 laser shots. The fits are all of excellent quality despite the numerous optical interferences encountered in heavily sooting flames. The highest nonresonant contribution clearly arises in the fuel jet, with significant but lesser nonresonant background observed elsewhere. These results are typical of fits in each of the three locations and show that the dual-pump CARS technique can provide reliable thermometry, even under the heavy soot loadings, complex fuel-rich chemical environment, and intense background luminosity encountered here.

Vertical-axis profiles of CARS-measured temperatures and LII-determined soot volume fractions are displayed in Fig. 11 for the fuel jet, the oxidizer jet, and the dormant Al-injection port at the burner center, as identified in the burner schematic in Fig. 1b and the LII data planes of Fig. 3. The temperature data represent the mean of 10 CARS measurements at each location, obtained from spectra that were averaged on the detector for 10 laser shots. The 2.25-mm length of the CARS probe volume prohibits resolution of the diffusion-flame structure so that the temperatures are spatially averaged across the core of the jets, although no obvious impact of density weighting bias is apparent in the spectra [39]. At all three locations, the temperature profile decays from its maximum with increasing height above the burner surface, which is to be expected as a result of radiative heat loss from in-flame soot. Temperatures in the N_2-rich gases above the central Al-particle injection port are much higher than in the outer fuel and oxidizer ports, presumably as a result of the lack of soot in this region of the burner. Vertical profiles of soot volume fraction show maximum soot loadings as high as 2 ppm for which CARS temperatures in the fuel jet are reliable. Soot loadings in the adjacent O_2/N_2 stream are an order of magnitude lower than in the fuel jet, with the time-averaged presence of soot resulting from low levels of flickering of the adjacent sooting fuel jets that increases with distance above the burner surface.

Similar vertical profiles of temperature and soot volume fraction along the centerline of the premixed C_2H_4/air flame are presented in Fig. 12. The CARS temperature measurements effectively capture the rapid temperature rise through the preheat and reaction zones, with a peak flame temperature near 1600 K achieved by ~10 mm above the burner surface, where measurable quantities of soot first begin to appear. At ~20 mm from the burner surface, the temperature begins to drop with increasing height above the burner,

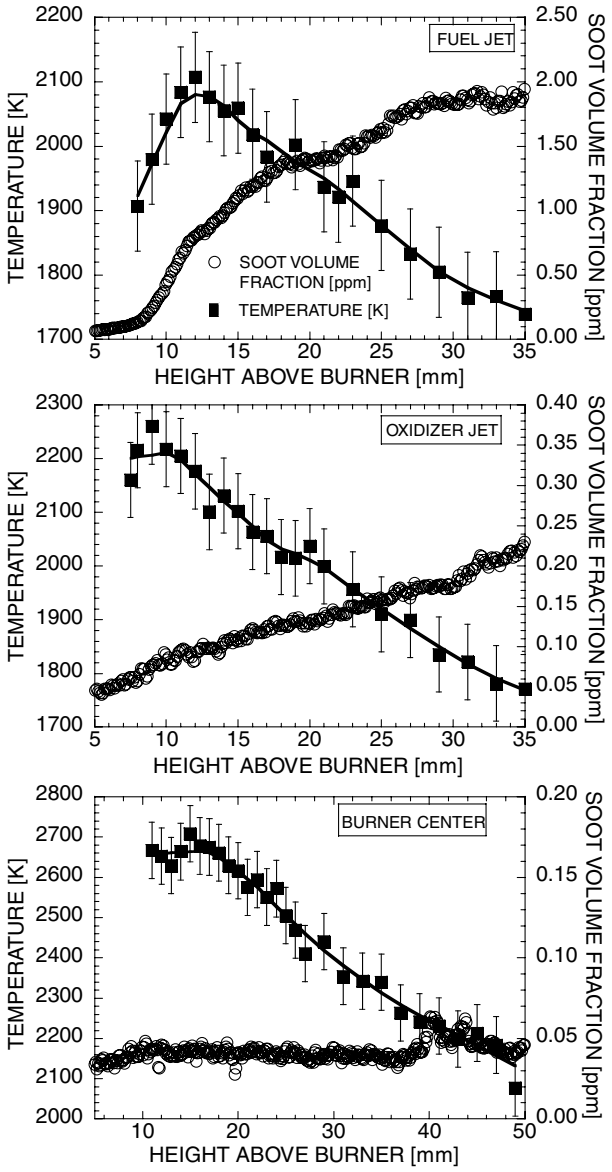

Fig. 11 CARS-measured vertical temperature profiles and LII-measured profiles of soot volume fraction in the N_2-diluted C_2H_2 fuel jet in which the highest sooting conditions occur, in the N_2/O_2 stream next to the fuel jet, and in the product-gas stream above a dormant Al-injection port. Measured data points are indicated by filled squares and open circles, and solid lines are a smooth curve passed through the temperature data and are representative of the temperature profile. Uncertainty in the soot-volume-fraction data is +20 to −40%.

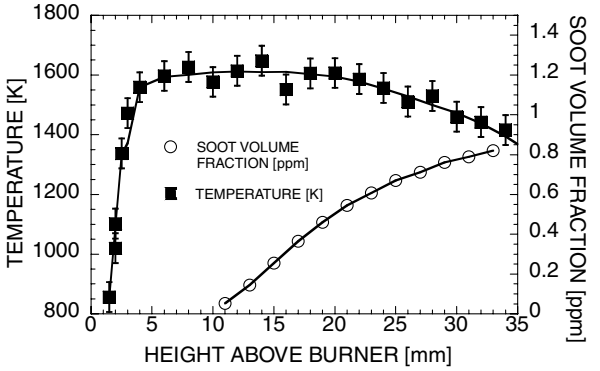

Fig. 12 CARS-measured vertical temperature profile alongside the light-extinction-measured profile of soot volume fraction acquired along the centerline of a fuel-rich premixed C_2H_4/air flame stabilized on a McKenna burner. Measured data points are indicated by filled squares and open circles, and solid lines are smooth curves passed through the temperature and soot data and are representative of the measured profiles. Uncertainty in the soot-volume-fraction data is estimated to be ±30%.

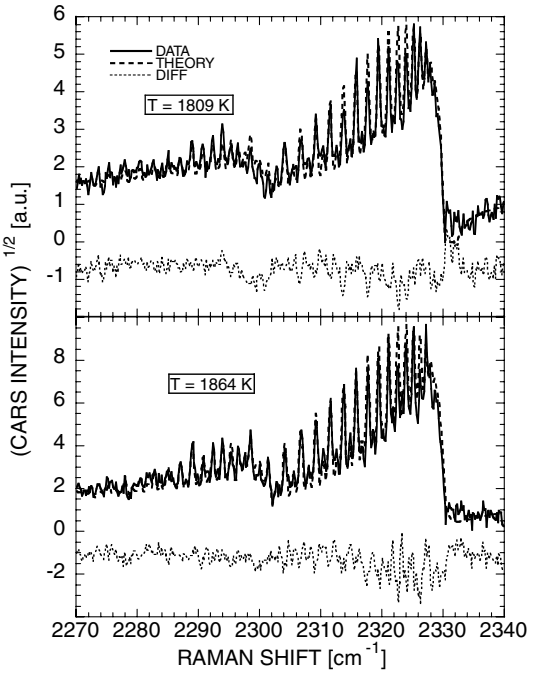

Fig. 13 Representative single-laser-shot dual-pump CARS spectra obtained from a heavily sooting region of a rich $C_2H_2/N_2/O_2$ array of diffusion flames. The pump-2 wavelength was 545 nm.

as would be expected with significant radiative heat loss as the soot volume loading increases.

The uncertainty in the shot-averaged CARS temperatures was estimated from two primary sources of error: 1) shift of the center frequency of the Stokes dye-laser output spectrum and 2) scatter associated with the fitting of CARS spectra that were averaged for 10 laser shots, which results from detector shot noise, imperfect background subtraction, and finite sampling of shot-to-shot mode-amplitude fluctuations in the Stokes laser output. Errors associated with theoretical modeling of the N_2 CARS spectra and with spatial averaging along the axis of the CARS probe volume were considered to be second order and were not included in the analysis. The center frequency of the Stokes dye-laser output spectrum was observed to shift by as much as 12.5 cm^{-1} over the course of the measurements in the $C_2H_2/N_2/O_2$ flames, the impact of which was quantified as ±50 K, based on repeat fits to CARS spectra that were normalized by different Stokes laser profiles taken immediately before and after each of the vertical scans. Scatter in the temperatures resulting from dye-laser mode noise, imperfect background subtraction, and detector shot noise was determined to be ±50 K, based on the observed variances of the 10-shot temperatures from their mean values. These two sources of random error were vector-summed to arrive at a composite uncertainty of ±70 K for the CARS temperatures presented in Fig. 11 and ±50 K for the temperatures in Fig. 12, because shifts in the dye-laser profile were not observed for the runs in the McKenna burner.

Potential for Single-Laser-Shot Measurements

The flames investigated here were largely steady and laminar in nature, which lends itself to the more accurate shot-averaged interrogation schemes used for the results presented thus far. Nonetheless, a small number of single-laser-shot CARS spectra were acquired in heavily sooting environments. The single-shot spectra were acquired at a height of $z = 45$ mm from the burner surface, at a

location above a C_2H_2 fuel port along the lateral at the lateral edges of the burner, where soot loadings were highest. The flow rates of C_2H_2, N_2, and O_2 were 4.8, 15, and 5 SLPM, respectively, which is significantly richer than for the shot-averaged CARS data presented earlier. Soot-volume-fraction data were not available for this operating condition, but the soot loading is surely in excess of the ~2-ppm peak values measured at this location under leaner conditions. This environment presents a significant challenge for single-shot CARS measurements, because a significant portion (~30%) of the spectra were discarded because the resonant N_2 CARS signature was overwhelmed by a breakdown-enhanced nonresonant component of the type shown in Fig. 9. Representative single-laser-shot spectra and their associated theoretical fits are presented in Fig. 13. The average temperature at this location was 1723 K, with a standard deviation of 167 K, or ~9.5% of the mean, observed in the ensemble of 70 single-shot measurements. At this location, the flame jets flicker in an unsteady fashion, which contributes some to the temperature spread in these single-shot data.

Conclusions

We extended the reported application space for dual-pump CARS thermometry to C_2H_2 fuel and to soot volume loadings as large as 2 ppm. This represents a significantly more heavily sooting and fuel-rich test of the dual-pump method than has previously been quantified. The wavelength of the dual-pump CARS signal was scanned from 482.4 to 497.7 nm by tuning the frequency of the pump-2 dye source. Coherent interference, which is intimately linked to the presence of soot, was observed to contaminate N_2 CARS spectra for signal wavelengths from 484 to 494 nm. This spectral region is typically thought to be "quiet," because it is off resonance with the C_2 Swan system. The interference in this case results from CARS processes in laser-produced C_2 and, potentially, from naturally occurring olefinic hydrocarbons. These interference signatures are on the order of the observed N_2 CARS or larger, and we surmise that the amplitude of the interference could be augmented by the ERE-CARS process. Two spectrally quiet regions were identified with pump-2 wavelengths near 544 nm and 560–563 nm, where dual-pump N_2 CARS signals with minimal coherent background could be obtained.

Enhanced nonresonant CARS signatures were also observed in the most heavily sooting regions of the C_2H_2-fueled flames investigated, which is similar in nature to earlier reports of interference resulting from particle-enhanced dielectric breakdown in coal-burning flames. The impact of breakdown did not significantly hinder analysis of shot-averaged spectra, but can overwhelm single-shot N_2 CARS signals in some cases.

Reliable temperature data were obtained from these heavily sooting flames using a pump-2 wavelength of 544.5 nm. The results show that the dual-pump CARS approach is a reliable tool for thermometry in heavily sooting flames, albeit with more restrictions on the spectral location of the N_2 CARS signal than previously realized. One notable consequence is that nitrogen CARS thermometry with simultaneous measurement of oxygen may be hampered, because the 1556 cm^{-1} Raman shift of O_2 is in close proximity to the coherent C_2 interference observed here. Spectrally shifted vibrational CARS of nitrogen is likely a viable alternative for thermometry because it shifts the N_2 CARS signal away from the C_2 Swan bands without creating a pump/Stokes separation that is Raman-resonant with C_2 or olefinic hydrocarbons.

Acknowledgments

This work was funded by the Sandia National Laboratories Engineering Sciences Research Foundation (ESRF) and the U.S. Department of Energy Campaign 6 programs. The authors would like to acknowledge Tom Grasser and Jaime Castaneda of Sandia for their help in the construction of the burner-facility positioning system and the Stokes dye laser used for the coherent anti-Stokes Raman scattering (CARS) measurements. We thank Chris Shaddix of Sandia for providing us with the results of his C_2 emission calculations, which were used to construct Fig. 5. We would also like to thank Frank Beyrau, Anna Malarski, Markus Weikl, and Thomas Seeger of the Universität Erlangen—Nürnberg for comments regarding interference in the CARS spectra and for sending us a copy of their unpublished work in [34]. Sandia is a multiprogram laboratory operated by Sandia Corporation, a Lockheed-Martin Company, for the U.S. Department of Energy's National Nuclear Security Administration under contract DE-AC04-94AL85000.

References

[1] Eckbreth, A. C., *Laser Diagnostics for Combustion Temperature and Species*, Gordon and Breach, New York, 1996.

[2] Hoinghaus, K. K., and Jeffries, J. B., *Applied Combustion Diagnostics*, Taylor and Francis, Philadelphia, 2002.

[3] Eckbreth, A. C., "CARS Investigations in Flames," *Seventeenth Symposium (International) on Combustion*, Combustion Inst., Pittsburgh, PA, 1977, pp. 975–983.

[4] Eckbreth, A. C., and Hall, R. J., "CARS Thermometry in a Sooting Flame," *Combustion and Flame*, Vol. 36, No. 1, 1979, pp. 87–98.
doi:10.1016/0010-2180(79)90048-8

[5] Farrow, R. L., Lucht, R. P., Flower, W. L., and Palmer, R. E., "Coherent Anti-Stokes Raman Spectroscopic Measurements of Temperature and Acetylene Spectra in a Sooting Diffusion Flame," *Twentieth Symposium (International) on Combustion*, Combustion Inst., Pittsburgh, PA, 1984, pp. 1307–1312.

[6] Hall, R. J., and Boedeker, L. R., "CARS Thermometry in Fuel-Rich Combustion Zones," *Applied Optics*, Vol. 23, No. 9, 1984, pp. 1340–1346.

[7] Herzberg, G., *Molecular Spectra and Molecular Structure*, 2nd ed., Van Nostrand, New York, 1950.

[8] Bengtsson, P. E., Aldén, M., Kröll, S., and Nilsson, D., "Vibrational CARS Thermometry in Sooting Flames: Quantitative Evaluation of C2 Absorption Interference," *Combustion and Flame*, Vol. 82, No. 2, 1990, pp. 199–210.
doi:10.1016/0010-2180(90)90098-C

[9] Greenhalgh, D. A., "RECLAS: Resonant-Enhanced CARS from C2 Produced by Laser Ablation of Soot Particles," *Applied Optics*, Vol. 22, No. 8, 1983, pp. 1128–1130.

[10] Eckbreth, A. C., Anderson, T. J., and Dobbs, G. M., "Conditional Sampling for Fuel and Soot in CARS Thermometry," *21st Symposium (International) on Combustion*, Combustion Inst., Pittsburgh, PA, 1986, pp. 1747–1754.

[11] Brackmann, C., Bood, J., Bengtsson, P. E., Seeger, T., Schenk, M., and Leipertz, A., "Simultaneous Vibrational and Pure Rotational Coherent Anti-Stokes Raman Spectroscopy for Temperature and Multispecies Concentration Measurements in Sooting Flames," *Applied Optics*, Vol. 41, No. 3, 2002, pp. 564–572.
doi:10.1364/AO.41.000564

[12] Beyrau, F., Seeger, T., Malarski, A., and Leipertz, A., "Determination of Temperatures and Fuel/Air Ratios in an Ethene-Air Flame by Dual-Pump CARS," *Journal of Raman Spectroscopy*, Vol. 34, No. 12, 2003, pp. 946–951.
doi:10.1002/jrs.1092

[13] Roy, S., Meyer, T. R., Lucht, R. P., Belovich, V. M., Corporan, E., and Gord, J. R., "Temperature and CO_2 Concentration Measurements in the Exhaust Stream of a Liquid Fueled Combustor Using Dual-Pump Coherent Anti-Stokes Raman Scattering (CARS) Spectroscopy," *Combustion and Flame*, Vol. 138, No. 3, 2004, pp. 273–284.
doi:10.1016/j.combustflame.2004.04.012

[14] Malarski, A., Beyrau, F., and Leipertz, A., "Interference Effects of C2 Radicals in Nitrogen Vibrational CARS Thermometry Using a Frequency-Doubled Nd:YAG Laser," *Journal of Raman Spectroscopy*, Vol. 36, No. 2, 2005, pp. 102–108.
doi:10.1002/jrs.1267

[15] Stricker, W., "Temperature Measurement," *Applied Combustion Diagnostics*, edited by K. K. Hoinghaus and J. B. Jeffries, Taylor and Francis, Philadelphia, 2002, pp. 155–193.

[16] Stricker, W., Luckerath, R., Meier, U., and Meier, W., "Temperature Measurements in Combustion—Not Only with CARS: A Look Back at One Aspect of the European CARS Workshop," *Journal of Raman Spectroscopy*, Vol. 34, No. 12, 2003, pp. 922–931.
doi:10.1002/jrs.1099

[17] Kröll, S., Bengtsson, P. E., and Nilsson, D., "Is Rotational CARS an Alternative to Vibrational CARS Thermometry?," *Applied Physics B, Photophysics and Laser Chemistry*, Vol. 51, July 1990, pp. 25–30.
doi:10.1007/BF00332320

[18] Lucht, R. P., "Three-Laser Coherent Anti-Stokes Raman Scattering Measurements of Two Species," *Optics Letters*, Vol. 12, No. 2, 1987, pp. 78–80.
[19] Santoro, R. J., and Shaddix, C. R., "Laser-Induced Incandescence," *Applied Combustion Diagnostics*, edited by K. K. Hoinghaus and J. B. Jeffries, Taylor and Francis, Philadelphia, 2002, pp. 252–286.
[20] Kearney, S. P., and Jackson, M. N., "Dual-Pump CARS Thermometry in Sooting Acetylene-Fueled Flames," 44th AIAA Aerospace Sciences Meeting and Exhibit, Reno, NV, AIAA Paper 2006-432, 2006.
[21] Williams, T. C., Shaddix, C. R., Jensen, K. A., and Suo-Anttila, J. M., "Measurement of the Dimensionless Extinction Coefficient of Soot Within Laminar Diffusion Flames," *International Journal of Heat and Mass Transfer*, Vol. 50, Nos. 7–8, 2007, pp. 1616–1630. doi:10.1016/j.ijheatmasstransfer.2006.08.024
[22] Dalzell, W. H., and Sarofim, A. F., "Optical Constants of Soot and Their Application to Heat-Flux Calculations," *Journal of Heat Transfer*, Vol. 91, No. 1, 1969, pp. 100–104.
[23] Shaddix, C. R., and Smyth, K. C., "Laser-Induced Incandescence Measurements of Soot Production in Steady and Flickering Methane, Propane, and Ethylene Diffusion Flames," *Combustion and Flame*, Vol. 107, No. 4, 1996, pp. 418–452. doi:10.1016/S0010-2180(96)00107-1
[24] Bethune, D. S., "Dye Cell Design for High-Power Low-Divergence Excimer-Pumped Dye Lasers," *Applied Optics*, Vol. 20, No. 11, 1981, pp. 1897–1899.
[25] Eckbreth, A. C., "BOXCARS: Crossed-Beam Phase Matched CARS Generation in Gases," *Applied Physics Letters*, Vol. 32, Apr. 1978, pp. 421–423. doi:10.1063/1.90070
[26] Palmer, R. E., "The CARSFT Computer Code for Calculating Coherent Anti-Stokes Raman Spectra: User and Programmer Information," Sandia National Labs., Rept. SAND89-8206, Livermore, CA, 1989.
[27] Hancock, R. D., Schauer, F. R., Lucht, R. P., and Farrow, R. L., "Dual-Pump Coherent Anti-Stokes Raman Scattering Measurements of Nitrogen and Oxygen in a Laminar Jet Diffusion Flame," *Applied Optics*, Vol. 36, No. 15, 1997, pp. 3217–3226.
[28] Xu, F., Sunderland, P. B., and Faeth, G. M., "Soot Formation in Laminar Premixed Ethylene/Air Flames at Atmospheric Pressure," *Combustion and Flame*, Vol. 108, No. 4, 1997, pp. 471–493. doi:10.1016/S0010-2180(96)00200-3
[29] Gordon, S., and McBride, B. J., "Computer Program for Calculation of Complex Chemical Equilibrium Compositions and Applications," NASA Lewis Research Center Rept. NASA RP-1311, Cleveland, OH, Oct. 1994.
[30] Hahn, J. W., and Lee, E. S., "Measurement of Nonresonant Third-Order Susceptibilities of Various Gases by the Nonlinear Interferometric Technique," *Journal of the Optical Society of America B (Optical Physics)*, Vol. 12, No. 6, 1995, pp. 1021–1027.
[31] Stephenson, D. A., "Raman Cross Sections of Selected Hydrocarbons and Freons," *Journal of Quantitative Spectroscopy and Radiative Transfer*, Vol. 14, No. 12, 1974, pp. 1291–1301. doi:10.1016/0022-4073(74)90098-3
[32] Ciajolo, A., D'Anna, A., Barbella, R., Tregrossi, A., and Violi, A., "The Effect of Temperature on Soot Inception in Premixed Ethylene Flames," *26th Symposium (International) on Combustion*, Combustion Inst., Pittsburgh, PA, 1996, pp. 2327–2333.
[33] Hanna, S. F., Kulatilaka, W. D., Arp, Z., Opatrny, T., Sculley, M. O., Kuehner, J. P., and Lucht, R. P., "Electronic-Resonance-Enhanced Coherent Anti-Stokes Raman Spectroscopy of Nitric Oxide," *Applied Physics Letters*, Vol. 83, No. 9, 2003, pp. 1887–1889. doi:10.1063/1.1604947
[34] Wendler, M., Guevara, G., Weikl, M. C., Sommer, R., Beyrau, F., Seeger, T., and Leipertz, A., "Comparison of Temperature Measurements in Non-Premixed Flames Using Emission Spectroscopy and CARS," *Third European Combustion Meeting (ECM2007)* [online proceedings], http://www.combustion.org.uk/ECM_2007/ecm2007_-papers/5-21.pdf [retrieved 7 October 2007].
[35] Beiting, E. J., "Coherent Interference in Multiplex CARS Measurements: Nonresonant Susceptibility Enhancement Due to Laser Breakdown," *Applied Optics*, Vol. 24, No. 18, 1985, pp. 3010–3017.
[36] Beiting, E. J., "Multiplex CARS Temperature Measurements in a Coal-Fired MHD Environment," *Applied Optics*, Vol. 25, No. 10, 1986, pp. 1684–1692.
[37] Hancock, R. D., Boyack, K. W., and Hedman, P. O., "Coherent Anti-Stokes Raman Spectroscopy (CARS) in Pulverized Coal Flames" *Advances in Coal Spectroscopy*, edited by H. L. C. Meuzelaar, Plenum, New York, 1992.
[38] Köylü, Ü. Ö., and Faeth, G. M., "Structure of Overfire Soot in Buoyant Turbulent Diffusion Flames at Long Residence Times," *Combustion and Flame*, Vol. 89, No. 2, 1992, pp. 140–156. doi:10.1016/0010-2180(92)90024-J
[39] Seeger, T., Weikl, M. C., Beyrau, F., and Leipertz, A., "Identification of Spatial Averaging Effects in Vibrational CARS Spectra," *Journal of Raman Spectroscopy*, Vol. 37, No. 6, 2006, pp. 641–646. doi:10.1002/jrs.1501

J. Gore
Associate Editor